Desalination, 61 (1987) 211–235
Elsevier Science Publishers B.V., Amsterdam — Printed in The Netherlands

Development of Wet–Dry Reversible Reverse Osmosis Membranes with High Performance from Cellulose Acetate and Cellulose Triacetate Blends

K. VÁSÁRHELYI*, J.A. RONNER, M.H.V. MULDER and C.A. SMOLDERS

Twente University of Technology, Department of Chemical Technology, P.O. Box 217, 7500 AE Enschede (The Netherlands) Tel. 3153899111; Telex 44200

(Received September 21, 1986)

SUMMARY

Wet–dry reversible membranes were prepared by a two-step coagulation procedure. A cast film containing a blend of cellulose acetate and cellulose triacetate as polymers, dioxane and acetone as solvents and maleic acid and methanol as additives was immersed consecutively in two aqueous coagulation baths, the first bath being kept at 0°C and the second at 60°C. The effects of casting solution composition and coagulation conditions on reverse osmosis performance and membrane morphology were examined. Light transmission measurements and demixing experiments have been carried out to investigate phase separation phenomena in this 6-component system. These experiments proved to be very helpful in explaining the reverse osmosis results.

High performance membranes have been obtained with salt rejections of more than 99% and permeation rates in the range of 10–12 l/m^2 h. These desalination properties, combined with a good wet–dry reversibility, make our membranes superior to reverse osmosis membranes hitherto produced.

INTRODUCTION

Since Loeb and Sourirajan developed a method to produce the asymmetric cellulose acetate (CA) membrane, there have been numerous attempts to prepare more efficient membranes for desalination from other polymeric materials. However, in most respects CA is still preferred as the polymer, yielding high performance and low cost reverse osmosis (RO) membranes. In spite of several good features, CA membranes have some drawbacks such as poor

*Present address: Hungarian Oil and Gas Research Institute, 8200 Veszprém, József Attila u. 34, Hungary.

0011-9164/87/$03.50

chemical and thermal resistance, fast biodegradability and strong flux decline under continuous operation.

Moreover, the fact that the conventional asymmetric CA membranes cannot be dried without being damaged presents numerous problems in storing, handling and installing these membranes and in shutting down the operating systems. Further complications arise because in the water, in which they have to be stored, these membranes are subject to biological attack.

Therefore it seemed of interest to investigate methods which could eliminate or at least diminish the problems concerning wet–dry irreversibility.

To avoid the problems of wet-storing, several processes for drying the wet membranes have been developed [1–4]. In each of these processes, water is removed from the pores by means of displacement (in several steps) by another nonsolvent in such a way as to minimize the capillary forces exerted on the pore walls at the final drying step. However, this multistep process must be repeated each time the membrane is dried (and re-wetted).

The problem could be solved by developing wet–dry reversible CA membranes, i.e. membranes that can be dried and re-wetted numerous times without any damage to the membranes, while no special treatment is required [5–10].

The Kesting dry method [8] uses complete evaporation of the solvent and nonsolvent from the cast film which contains CA as the polymer. The solvent has a lower boiling point than the nonsolvent. Using CA with 39.4–40.0% acetyl content, a dry asymmetric membrane can be obtained with 96% salt rejection and a flux of 20 l/m^2 h.

In the UCLA method [9] the cast film consisting of CA, acetone and formamide is allowed to evaporate for 2–60 s and then immersed in a water bath at 30–80 °C for 2–5 min. After drying, the membrane has a rejection of 99% and a flux of about 20–30 l/m^2 h.

In the Wafilin patent [10] the casting solution contains CA, acetone (Ac), dioxane (Dio), methanol (Me) and maleic acid (MA). After casting, the film was allowed to evaporate for 30 s, then immersed in water at 0 °C for 15 s, removed, allowed to stand for 10 s and then immersed in water at 50 °C, giving a membrane with a salt rejection of about 95% and fluxes in the range of 10–30 l/m^2 h.

WET-DRY REVERSIBILITY

The structure of a traditional asymmetric CA membrane shows that the sublayer directly beneath the dense toplayer (skin) contains pores with an average diameter of about 0.1 μm or even less. Upon drying, the pores gradually lose their original liquid (water) content thereby creating capillary forces (Fig. 1).

According to the Laplace-equation, these capillary forces are inversely pro-

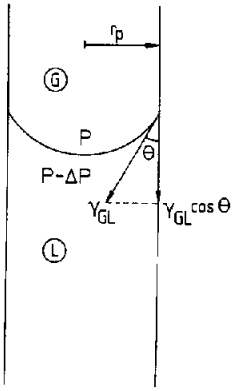

Laplace: $\Delta P = \frac{2\gamma_{GL}\cos\theta}{r_p}$

r_{pore} (μm)	ΔP (atm)
1	1
0.1	10
0.01	100

(for $2\gamma_{GL}\cos\theta$ = 100 mN.m^{-1})

Fig. 1. Capillary phenomena: r_p=pore radius (m), θ=liquid-solid contact angle, γ_{GL}=surface tension of the gas/liquid interface (N m^{-1}), P=pressure (N m^{-2}).

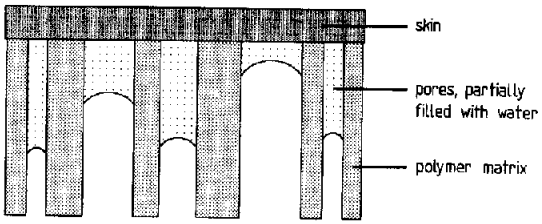

Fig. 2. Schematic representation of the membrane during drying.

portional to the pore radius. These forces can break the polymer matrix between pores with unequal dimensions, destroying the original structure and thereby adversely affecting the performance of the membrane. The weaker the polymer matrix between the pores, the smaller the capillary forces that are able to break the matrix (Fig. 2).

Consequently, the crucial parameters in wet–dry reversibility are the pore size and size distribution, the mechanical properties of the polymer matrix and the porosity (i.e. the number of pores per unit volume).

We have assumed that we have the possibility to direct two crucial parameters from the above listed. We hope to increase the pore size directly below the toplayer by using casting solutions containing additives which are known as pore-forming materials and by using coagulation conditions which are supposed to favour the pore-growth after the skin has already been formed. The strength of the membrane matrix is the second parameter that we can possibly direct using CA polymer types with properties which favour structural regularity and crystalline order.

TWO BATH COAGULATION PROCESS

Asymmetric membranes are classically produced by the so-called phase-inversion process [11]. In this process a homogeneous polymer solution is cast

as a thin film followed by the immersion of the film in a nonsolvent coagulation bath. During immersion there is a rapid exchange of solvent and nonsolvent which leads to the formation of an asymmetric membrane consisting of a dense toplayer and a porous substructure. During the membrane formation two types of demixing processes can be distinguished [12]:

(a) Formation of aggregates: the solution demixes as a result of aggregation of the polymer molecules (possibly induced by crystallization).

(b) Liquid–liquid (l–l) phase separation: the polymer solution separates into two liquid phases (through nucleation and growth of one of the phases).

The porous substructure is usually the result of l–l phase separation which occurs by nucleation and growth of the polymer-poor phase until aggregate formation in the concentrated phase stops this process.

Thus, for producing pores in the substructure directly below the toplayer larger than those in the traditional wet membranes, the formation of too many nuclei of the diluted phase should be prevented and the growth of these nuclei should be favoured.

A two-step coagulation procedure has been suggested [10,13] to meet this requirement. Instead of using only one coagulation bath (at low temperature) followed by a curing procedure (at a temperature above the glass transition), two coagulation baths are used consecutively. The film remains for only a short time in the first (low temperature) bath, permitting the skin to be formed and the nucleation of the polymer-poor phase to start. Immediately after the first bath the film is put in the second warmer bath for a longer period of time, where the growth of nuclei is favoured and the aggregate formation of the concentrated phase is delayed at the same time. In this way the nuclei can grow further before solidification stops the process.

CASTING SOLUTION FORMULATION

As mentioned above, changing the casting solution formulation may affect two crucial parameters of wet–dry reversibility, namely the pore size and the strength of the polymer matrix.

We have used a CA–cellulose triacetate (CTA) blend as the polymer, in which the CTA had an acetyl content larger than 42.3% and a rather high average molecular weight ($M_w \approx 200{,}000$). Both the increased degree of acetyl substitution and the high molecular weight lead to increased structural regularity (crystallinity) and hence improved mechanical strength [14]. With CTA, salt rejections higher than 99% can be achieved, which is not possible with CA only. Furthermore, the fact that CTA is superior to CA in respect to biological and chemical stability [15] means that it is even more attractive to use CTA in the blend.

In general, acetone is used as a solvent for CA, but because of the limited solubility of CTA in this solvent it is necessary to include another solvent in

the casting solution. The acetone (Ac)–dioxane (Dio) solvent mixture has been found suitable for the blend [16].

Two additives have been introduced to the casting solution, Me and MA. These additives are supposed to act as a nonsolvent and a swelling agent respectively, and are frequently used in membrane-forming systems [10, 16–18]. They allow a high degree of membrane swelling and thus permit a high water flux [16] and a high salt rejection simultaneously. The use of a swelling agent seemed especially important in the case of the CA–CTA blend because the absolute equilibrium water content (degree of swelling) of the membrane decreases with increasing acetyl content, which also leads to decreasing permeability [15].

The search for appropriate casting solution compositions for making membranes with optimal performance characteristics has proceeded mostly by means of experimental trial and error procedures. Obviously, the use of a 6-component casting solution, described above, is the result of such a procedure. Although each of these components serves a more or less well defined purpose, it is not quite clear in which way they influence the membrane structure. Fundamental knowledge about this question might lead to a more efficient optimization procedure. Therefore we will also deal with some fundamental aspects of this multicomponent system.

EXPERIMENTAL

Composition of the casting solutions

The so-called basic casting solution (No. 1) contained 7% (w/w) CTA, 7% (w/w) CA, 3% (w/w) MA, 7% (w/w) Me and as the solvent, a mixture of Dio and Ac in the ratio of 5:3.

To study the effect of the components on RO performance we varied the casting solution composition in such a way that the concentration of only one of the components was changed at the same time. In this way we obtained ten casting solutions of different compositions including the basic solution (see Table I). The No. 11 casting solution contained neither MA nor Me.

In addition we made casting solution (No. 12) according to the Manjikian–Loeb method [19]. This solution was composed of 25% (w/w) CA, 30% (w/w) formamide (Form) and 45% (w/w) Ac.

CA obtained from Eastman-Kodak (E 398–3–6) and CTA (from Janssen Chimica) were dried before use. According to HPLC-LALLS, CA had a $\bar{M}_N$, $\bar{M}_W$ of 24,400 and 42,100 respectively and CTA had a $\bar{M}_N$, $\bar{M}_W$ of 122,500 and 205,800 respectively. Reagent grade Dio, Ac, Me, Form and MA were used without further purification.

TABLE I

Composition of casting solutions

Casting solution No.	Concentrations of components in the casting solution in % w/w						
	CTA	CA	MA	Me	Dio	Ac	Form
1	7	7	3	7	47.5	28.5	—
2	9	9	3	7	45.0	27.0	—
3	10	10	3	7	43.7	26.3	—
4	7	7	—	7	49.4	29.6	—
5	7	7	5	7	46.2	27.8	—
6	7	7	6	7	45.6	27.4	—
7	7	7	3	—	51.9	31.1	—
8	7	7	3	14	43.1	25.9	—
9	7	7	3	7	61.7	14.3	—
10	7	7	3	7	76.0	—	—
11	7	7	—	—	53.7	32.3	—
12	—	25	—	—	—	45	30

Membrane preparation — casting and coagulation conditions

The solutions were hand-cast on a glass plate using a casting knife with a thickness of 0.2 mm. The casting speed was about 4 cm/s. The applied coagulation conditions are summarized in Table II.

In the basic coagulation procedure (symbol B) evaporation was avoided as

TABLE II

Coagulation conditions

Coagulation condition	Evaporation time (t_0) (s)	First bath		Second (curing) bath	
		Temperature T_1 (°C)	Residence time (t_1) (min)	Temperature T_2 (°C)	Residence time (t_2) (min)
B	—	0	5	60	10
B1	—	10	5	60	10
B2	—	20	5	60	10
B3	—	—	—	60	10
B4	—	0	0.5	60	10
B5	—	0	1	60	10
B6	—	0	2	60	10
B7	—	0	5	—	—
M	30	0	>60	85	10
J	6	60	5	—	—

far as possible. Coagulation was performed in two water baths. The temperature of the first bath was 0 °C and the residence time 5 min. Immediately after the first bath a second bath was used at 60 °C for 10 min.

To examine the effect of the coagulation conditions on the RO performance of the membranes, we varied the temperature of the first bath (symbols B1, B2), the residence time of the films in the first bath (symbols B3, B4, B5, B6) and eliminated the second bath completely (symbol B7). These variations have been applied to the basic casting solution.

In addition, we used the Manjikian–Loeb coagulation process [19] for the No. 1 and 12 casting solutions, and the UCLA method [9] for the No. 1 and 12 casting solutions. In the Manjikian–Loeb process (symbol M) there is an evaporation time of 30 s, followed by immersion of the film in a water bath of 0 °C for more than 60 min and finally a curing bath at 85 °C is used for 10 min. The UCLA method (symbol J) used an evaporation time of 6 s and a coagulation bath at 60 °C for 5 min. The latter process is expected to result in a wet–dry reversible membrane if used for the No. 12 casting solution [9].

Reverse osmosis experiments

The membranes were tested without further treatment in the wet state, then dried in air and tested again.

RO experiments were carried out in a cross-flow testing device at 20 °C, a pressure of 3 MPa and a feed concentration of 3000 ppm NaCl.

The concentration of NaCl in the feed and the permeate were determined by conductivity measurements.

Demixing experiments

In order to determine the compositions at which the system separates into different phases (e.g. the l–l demixing gap and the aggregate formation transition) we prepared solutions with different water contents. After homogenization at temperatures up to 80 °C, these solutions were kept at room temperature. At the appearance of a two-phase system, with at least one clear phase to be isolated (e.g. by centrifugation), l–l demixing was assumed to have taken place.

The role of MA and Me in our system was studied in more detail. In l–l demixed solutions, the distribution of MA across both phases was investigated by titration of the diluted phase. Preferential occurrence of MA in one of the phases obtained during membrane formation, was established by means of coagulation experiments, followed by titration of the coagulation bath. Further, swelling experiments were carried out to reveal the influence of MA when present in the polymer-rich phase.

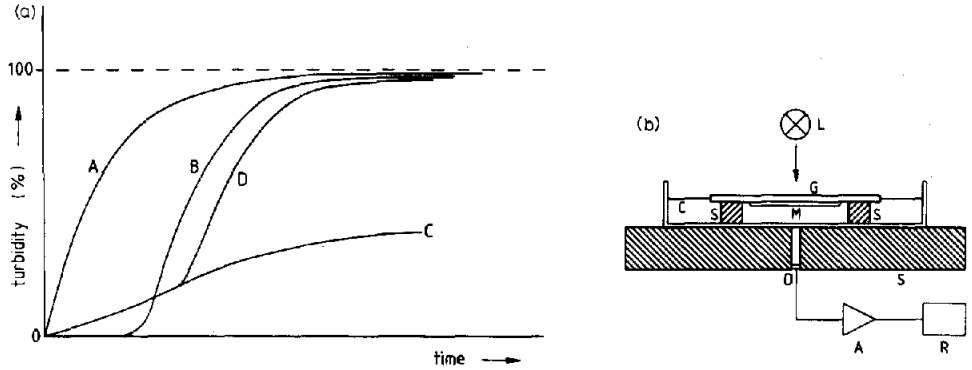

Fig. 3a. Light transmission measurements: turbidity–time relations during membrane formation. Fig. 3b. Light transmission measurements: experimental set up. L, light source; G, glass plate; M, nascent membrane; C, coagulation bath; S, support; D, photodiode; A, amplifier; R, recorder.

Light transmission experiments [20]

The light transmission method for studying the membrane formation mechanism will be explained in more detail.

In principle, the turbidity of the nascent membrane is measured as a function of time (Fig. 3a). Here, turbidity is defined as 100%–transmittance.

Measurements are carried out using a transparent coagulation bath container and membrane support plate, a light source above the bath and a photodetector below the bath. The photodetector signal is amplified and recorded. Fig. 3b shows a schematic representation of this equipment.

In Fig. 3a, curves A–D denote different turbidity–time relations that can be observed during membrane formation. Curves A and B are obtained when, after immersion, l–l demixing occurs, causing a structure which strongly scatters the incident light (i.e., many large inhomogeneities per unit volume). In the membrane forming system, represented by curve A, l–l demixing begins immediately after immersion. Curve B is obtained for systems where a certain period of time is required before the exchange of solvent and nonsolvent (by diffusion) leads to a metastable composition in the polymer solution, causing l–l demixing to be delayed [21].

In curves C and D inhomogeneities are being formed immediately after immersion. However, during the first seconds the degree of optical anisotropy remains significantly smaller than in curve A. We consider these inhomogeneities to be formed by a polymer solidification process which we consider to be due to aggregate formation. In this process polymer-rich clusters (aggregates) are formed within a composition range that does not yet permit l–l demixing to occur. As a result of aggregate growth, a solid, porous structure is formed. When aggregate formation begins at a high polymer concentration, only a low

degree of porosity can be obtained. The density will be large enough to offer a significant flux resistance, especially when this structure constitutes a thicker layer in the membrane cross-section. The occurrence of aggregate formation may even prevent l–l demixing from occurring , causing the membrane to be almost transparent (low turbidity level, curve C). In curve D, the bend indicates the time at which l–l demixing starts, following aggregate formation, at a point in the film below the aggregated toplayer.

Polymer solidification during membrane formation may also occur without inhomogeneities being formed. In this case, an amorphous, homogeneous and extremely dense structure is the result. We consider the skin of RO membranes to be formed by such a process, due to the extremely high polymer concentration which develops almost immediately after immersion in this part of the polymer film.

Scanning electron microscopy (SEM)

The membranes used for the SEM experiments were fractured at liquid nitrogen temperature and sputtered with gold. Cross-sections were investigated using a Jeol JSM-35CF scanning electron microscope.

RESULTS AND DISCUSSION

Wet–dry reversibility

The difference in RO membrane performance before and after drying was adopted as a measure for wet–dry reversibility. Thus, the membranes obtained were firstly tested in a wet state for 24 h. After a 2 d drying period they were re-wetted and tested again. The results, i.e. the rejection and flux values of the membranes before and after drying are summarized in Table III.

The membranes 6/B, 12/B and 12/M could not be tested after drying because of very strong deformations (shrinkage, curling, etc.). All other membranes kept their original shape and size after drying and they could be handled easily in the dry state.

As can be seen from Table III, the RO performance of the membranes changed after drying: the rejection increased and the flux decreased. In several cases these changes were significant. It is very difficult to decide which discrepancies can still be tolerated, i.e., which membranes can still be regarded as wet–dry reversible. To solve this problem, first we have to consider the effect of wet–dry irreversibility on RO performance.

If the capillary forces are able to deform the polymer matrix between the pores, the opposite sides of the pore walls will make contact with the result that the pore disappears. This leads to a loss of porosity in the substructure and hence a decrease in the water flux, while the rejection may remain con-

TABLE III

RO performances of the membranes before and after drying. R and J are the rejection and the flux, respectively; subscripts w and d refer to the original wet state and the performance after a wet-dry cycle, respectively; $\Delta R = (R_d - R_w)/R_w$; $\Delta J = (J_d - J_w)/J_w$

Membrane[a]	Main characteristic of membrane[b]	R_w (%)	J_w (l/m^2 h)	R_d (%)	J_d (l/m^2 h)	ΔR (%)	ΔJ (%)	Wet-dry reversibility
1/B	Basic configuration	98.9	11.3	99.0	10.7	0.1	−5.4	W-D
2/B	Polymer = 18% w/w	98.6	11.0	99.0	10.4	0.4	−3.6	W-D
3/B	Polymer = 20% w/w	99.0	10.0	99.1	9.6	0.1	−4.0	W-D
4/B	MA = 0% w/w	98.5	7.0	99.2	6.3	0.7	−10.0	W-D
5/B	MA = 5% w/w	96.6	4.4	97.2	3.9	0.6	−11.3	W-D
6/B	MA = 6% w/w	97.1	26.5	deformed	—	—	—	W
7/B	Me = 0% w/w	98.7	6.0	99.2	5.4	0.5	−10.0	W-D
8/B	Me = 14% w/w	96.8	4.1	97.7	3.9	0.9	−4.8	W-D
9/B	Dio : Ac = 6.5 : 1.5	81.9	15.0	84.7	13.3	3.4	−11.3	W-D
10/B	Dio : Ac = 8 : 10	62.3	21.1	66.2	18.6	6.2	−11.8	W-D
11/B	Me and MA = 0%	81.0	11.5	87.1	7.9	7.5	−31.3	D
12/B	Manj.sol.	58.3	111.4	deformed	—	—	—	W
1/B1	$T_1 = 10$ °C	94.6	13.3	96.2	11.9	1.7	−10.5	W-D
1/B2	$T_1 = 20$ °C	91.9	16.5	93.2	14.3	1.4	−13.3	W-D
1/B3	$t_1 = 0$ min	74.5	25.2	75.3	20.1	1.7	−20.2	D
1/B4	$t_1 = 0.5$ min	98.5	13.4	98.9	11.9	0.4	−11.2	W-D
1/B5	$t_1 = 1$ min	98.3	11.7	98.8	11.4	0.5	−2.5	W-D
1/B6	$t_1 = 2$ min	98.5	11.9	98.9	10.8	0.4	−9.2	W-D
1/B7	$t_2 = 0$ min	91.7	31.3	98.0	10.5	6.9	−66.4	D
1/M	Manj.proc.	99.0	7.7	99.1	7.1	0.1	−7.7	W-D
1/J	UCLA proc.	75.4	24.7	76.3	19.1	1.1	−22.6	D
12/M	Manj.sol.	—	—	—	—	—	—	
	Manj.proc.	99.0	1.9	deformed	—	—	—	W
12/J	Manj.sol.	—	—	—	—	—	—	
	UCLA.proc.	94.2	11.0	96.6	9.1	2.5	−17.2	D

[a]The number before the stroke refers to the casting solution and the letter or letter-number combination after the stroke refers to the coagulation process.
[b]The main characteristic is the parameter which was changed compared to the basic configuration.

stant. In the worst case, the asymmetric pore size distribution may cause a strong capillary force gradient to occur across the membrane, leading to severe membrane deformation.

It can be assumed that the structure of the membranes 6/B, 12/B and 12/M has been damaged upon drying. Since in all other cases the flux decline was accompanied by an increased rejection, we think that these differences in RO performance before and after a wet-dry cycle can be due to the shrinkage of the skin without serious damage occurring in the membrane substructure. (The drying seems to act in the same way as the heat curing procedure for CA membranes.)

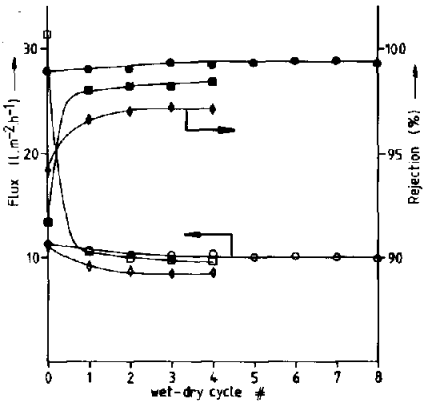

Fig. 4. Wet-dry reversibility: RO membrane performance after several wet-dry cycles. ○, 1/B; □, 1/B7; ◇, 12/J; open symbols = flux; closed symbols = rejection.

Yet, within the group of membranes that could be tested we should distinguish between membranes which showed a flux decline of only 5% after drying and membranes with a 60% decline in flux. For this reason we arbitrarily created 3 categories of wet-dry reversibility. Membranes with a flux decrease of about 10% or less were regarded as wet-dry reversible (W-D); those which showed a stronger flux decline, but still had visually excellent wet-dry properties were considered as dry-storable membranes (D) and finally, the membranes which deformed upon drying and hence could not be used after having been dried, were taken as wet membranes (W).

For the membranes 1/B, 1/B7 and 12/J, RO performance was measured after repeated drying and re-wetting (wet-dry cycles). The 1/B membrane was subjected to 8 and the 1/B7 and 12/J membranes to 4 wet-dry cycles (see Fig. 4). The 1/B7 and 12/J membranes were chosen for this experiment because the former one showed the largest flux decrease after drying, and the latter one was made according to the UCLA patent and was known as a wet-dry reversible membrane. However, as can be seen from Table III, the UCLA method yielded dry-storable but not wet-dry reversible RO membranes according to our classification. Disregarding the first cycle, i.e. from the original wet state to the first dry state, the flux decline during the test remained less than 10% for all three membranes.

Reproducibility of membranes

Besides the wet-dry reversibility and high performance, the circumstances which favour a good reproducibility of membrane fabrication are important.

For this purpose we made 12 membrane pieces from each of the solution/process combinations mentioned in Table III. After examination under trans-

TABLE IV

Reproducibility of membrane fabrication

Degree of reproducibility: $RD = R_{max} - R_{min}$				
0-1	1-2	2-3	5-7	15-16
2/B, 3/B 1/M, 12/M[a]	1/B, 4/B, 5/B, 6/B[a] 7/B, 8/B 1/B1, 1/B5 1/B6, 12/J	1/B2	11/B, 12/B[a] 1/B3, 1/B4 1/B7, 1/J	9/B, 10/B

[a]In these cases the rejection values refer to the wet-state.

mittant light, six of them were selected and tested simultaneously. The absolute difference between the maximum and the minimum rejection values obtained for these six membranes was chosen as a degree of reproducibility ($RD = R_{max} - R_{min}$), the rejection being more sensitive to imperfections than the flux. According to the degree of reproducibility, the membranes were divided into five categories (see Table IV), the lowest *RD* value indicating the most reproducible membranes.

Some changes could be observed from these experiments. With increasing polymer content, increasing Me content and decreasing coagulation temperature respectively, reproducibility improved. Reproducibility remained the same upon increasing the MA concentration and upon varying the residence time in the first bath from 1 to 5 min. When the residence time in the first bath was 30 s and zero respectively, the reproducibility worsened compared to the basic procedure (*RD* became 7 instead of 2) and wavelines could be observed on the membrane surfaces. The reproducibility of the membranes made without a second bath was also worse compared to the basic membrane.

In the case of a Dio:Ac ratio of 6.5:1.5 and 8:0 the reproducibility became very poor ($RD = 16$) and a huge amount of macrovoids could be observed in the membranes. When we omitted both MA and Me from the casting solution, the reproducibility was much poorer than when only one of them was omitted and the formation of pinhole size voids could not be avoided during casting.

The effect of coagulation conditions on the RO performance

The effect of coagulation temperature

With increasing temperature in the first bath (see 1/B, 1B1, 1B2), the rejection decreased from 99.0 to 93.2% and the flux increased from 10.7 to 14.3 l/m^2 h. If we assume that the 1/B3 membrane (without first bath) can be regarded as if it had first been coagulated at 60°C, the increase in temperature from 20

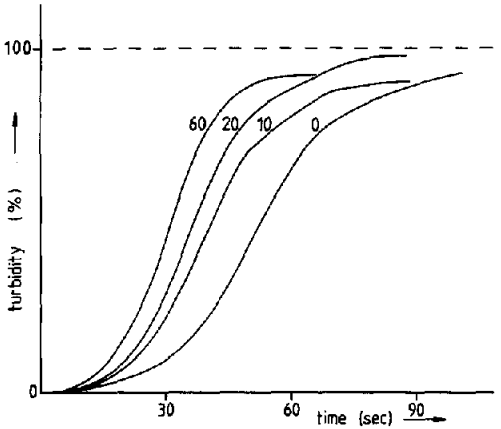

Fig. 5. Light transmission measurements: influence of coagulation bath temperature. Casting solution: No. 1 (basic solution). Temperatures in °C.

to 60 °C shows an even more dramatic decrease in the rejection (from 93.2 to 75.3%). Both the rejection decrease and the flux increase indicate that the skin becomes less compact with increasing coagulation temperature.

The light transmission curves (Fig. 5) show that the l–l demixing starts earlier and proceeds faster when the temperature is raised. An earlier start of l–l demixing implies nucleation at a smaller distance below the skin. Secondly, the increased rate of turbidity increase can be due to the enhanced growth of diluted phase nuclei. The result of both effects, i.e. a decrease of the toplayer thickness and larger pores upon raising the coagulation temperature, can be observed clearly in the SEM pictures (Fig. 6). The combination of large pores and a thin toplayer, obtained at high coagulation temperatures, may increase the possibility for small imperfections in the skin to form holes. This might explain the high flux and low rejection of the 1/B3 membrane (coagulated at 60 °C).

The effect of residence time of the film in the first bath

When the residence time in the first bath was changed from 30 s to 5 min (1/B4, 1/B5, 1/B6, 1/B) the rejection remained practically the same and the flux decreased somewhat which can be due to the thickening of the skin at the same compactness. In the SEM pictures we could not observe any difference between these membranes which is not surprising considering the very small differences in the RO performance and the impossibility of determining skin thicknesses with the SEM. The case of zero residence time in the cold bath (i.e. one bath coagulation at 60 °C, membrane 1/B3) has been discussed in the previous section.

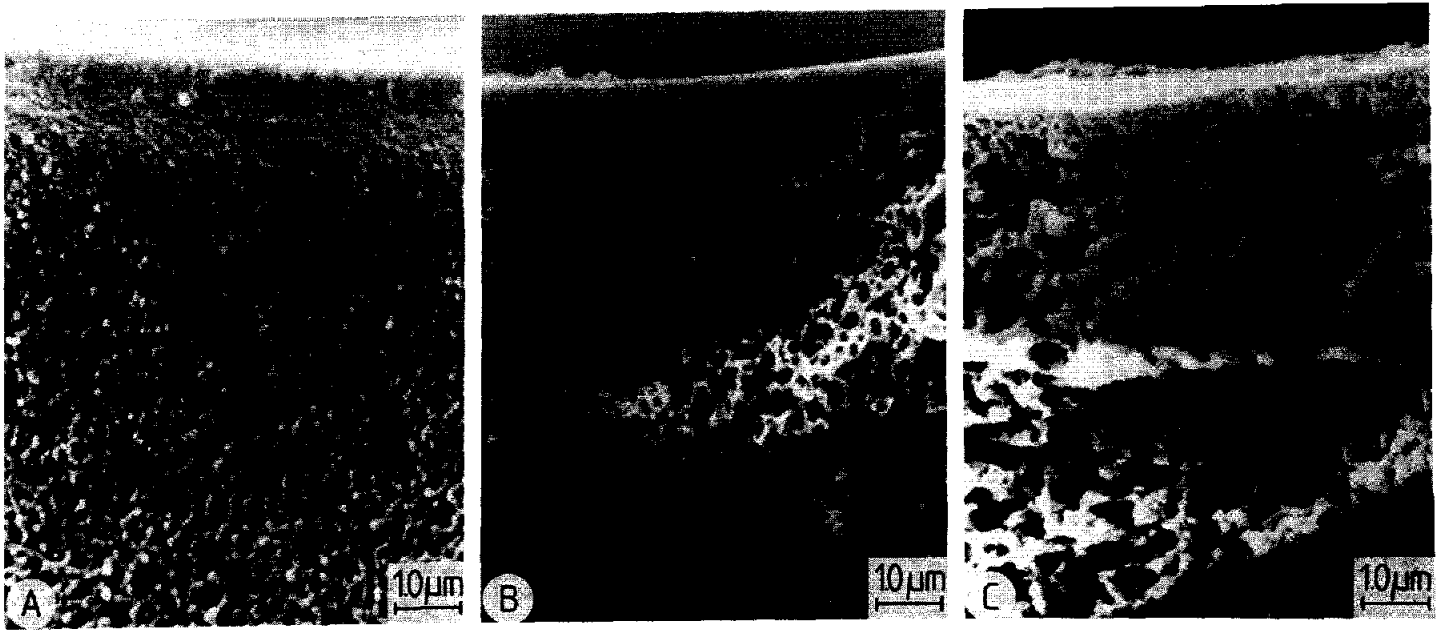

Fig. 6. SEM cross-sections: influence of coagulation bath temperature. Casting solution: No. 1 (basic solution). A, 0°C; B, 20°C; C, 60°C.

The effect of the second bath

The difference in RO performance between the membranes 1/B and 1/B7 (original wet state; with and without second bath, respectively) is very large. Using the second bath, membranes were obtained which had a much lower flux and a much higher rejection. From this it can be concluded that the second bath has a remarkable heat curing effect. The presence of solvent in the polymer film may have lowered the glass transition temperature of the system, thus permitting curing phenomena to occur at a relatively low temperature (60 °C). Secondly, diffusion and demixing processes will proceed in the second bath. Consequently, the second bath may also have a pore-enlarging effect.

After drying, the 1/B7 membrane shows about the same rejection (98–99%) and flux (10–11 l/m^2 h) as the 1/B membrane. As we pointed out earlier, drying appears to act in a similar way as heat curing, as is the case for the use of the second bath. However, the drying process is considerably more difficult to control and therefore leads to a poor reproducibility compared to the use of a second bath (see Table IV).

Comparison of different coagulation processes

We prepared membranes from the basic casting solution (No. 1) and the Manjikian–Loeb casting solution (No. 12) by using the two-bath (B), the Manjikian–Loeb (M) and the UCLA coagulation process (J). Casting solution compositions, coagulation conditions and RO data can be found in Tables I, II and III, respectively.

For the *basic casting solution*, both the two-bath and the Manjikian–Loeb process produced wet–dry reversible membranes (1/B and 1/M) with a high salt rejection (99%) and good reproducibility. Fluxes were 10.7 and 7.1 l/m^{2}h for the 1/B and 1/M membrane, respectively. The significantly lower flux obtained with the 1/M membrane, suggests a lower degree of porosity in the intermediate layer (in between the skin and the sublayer) of this membrane. This is confirmed by SEM photographs. Obviously, the combination of a curing step at 85 °C and an evaporation step is responsible for the formation of a very dense structure, when applied to the basic casting solution.

Using the *Manjikian–Loeb casting solution*, the two-bath process yielded a wet-storable membrane (12/B) with a very poor rejection (58.3%) and a very high flux (111.4 l/m^2 h). With the Manjikian–Loeb coagulation process, the membrane (12/M) was also wet-storable, but the rejection was high (99%) accompanied by an extremely low flux (1.9 l/m^2 h). We can conclude that for the Manjikian–Loeb casting solution, the two-bath process creates a structure which is too open. Omitting the evaporation step prevents a dense skin from being formed (poor rejection) while additionally the curing effect is also too weak. The Manjikian–Loeb coagulation process yields a dense skin, but the intermediate layer is also very dense. Obviously, the curing step involved is too strong (for both the basic and the Manjikian–Loeb casting solution).

Finally, the UCLA process, applied to the basic casting solution, yielded a dry-storable membrane (1/J) with a very poor rejection (76.3%). The resem-

blance with the 1/B3 membrane (see Table III) is clear; actually, the B3 and J procedures are practically identical (Table II). For the Manjikian–Loeb casting solution, the UCLA process is expected to give a wet–dry reversible membrane with a rejection of 99% and flux of about 20–30 l/m^2 h [9]. However, the membrane we obtained (12/J) had a rejection and flux of only 96.6% and 9.1 l/m^2 h respectively, the membrane being only dry-storable.

We can conclude that the two-bath process, applied to the basic casting solution, yields wet–dry reversible membranes with a relatively good RO performance.

Effects of the casting solution composition

The effect of polymer concentration

The total polymer concentration in the casting solution was varied from 14 to 20% (w/w). At increasing polymer concentration, the flux decreases while the rejection remains constant. This might be explained by an increased skin thickness (at the same skin density) at higher polymer concentration.

The effect of the Dio:Ac ratio

The solvent mixture composition (i.e. the Dio:Ac ratio) has been varied from 5:3 to 8:0, representing 62.5% to 100% (w/w) Dio, respectively. This leads to a flux increase (80%) together with a dramatic rejection decrease (33%). Rejection data show poor reproducibility.

Light transmission experiments (Fig. 7) show a more rapid initial turbidity increase with 100% (w/w) Dio as the solvent (curve 10), indicating an increased occurrence of aggregate formation. In both cases l–l demixing starts at an early stage. From this curve we might expect a porous substructure and an aggregated layer directly below the skin. Scanning electron micrographs (Fig. 8, plate B) indeed show such a structure. Considering this structure we would expect a higher rejection than we have actually obtained. Aggregate formation may even have caused the skin to become more porous. A second reason could be the occurrence of macrovoids (observed by examination under transmittant light). These imperfections offer only weak support for the skin, which will break under pressure at the weakest points, causing a low rejection. The random distribution of weakest points accounts for the poor reproducibility.

The rapid formation of macrovoids at the onset of l–l demixing, followed by the much slower development of a finely porous substructure, might explain the typical shape of the light transmission curve obtained for 100% Dio (Fig. 7, curve 10).

The effect of additives

The Me content of the casting solution varied from 0 to 14% (w/w). Within this range, increasing the Me concentration causes the rejection to decrease

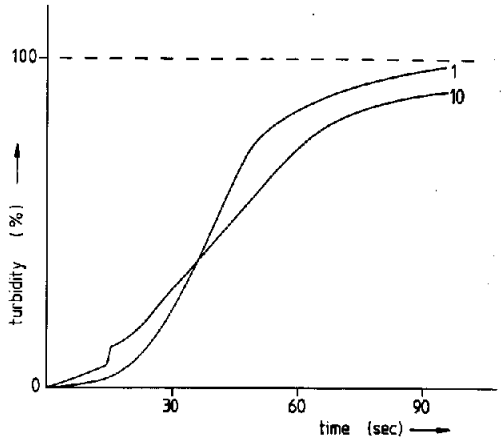

Fig. 7. Light transmission measurements: influence of solvent mixture composition. Numbers refer to the casting solutions (see Table I). 1, Dio:Ac ratio of 5:3 (basic solution); 10, Dio:Ac ratio of 8:0.

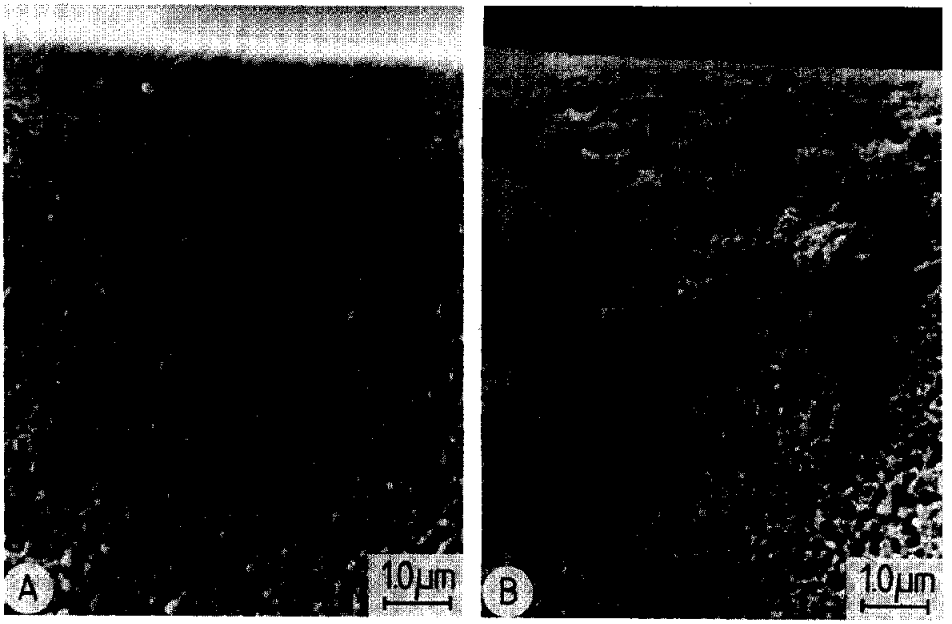

Fig. 8. SEM cross sections: influence of solvent mixture composition. A, Dio:Ac ratio of 5:3 (basic solution); B, Dio:Ac ratio of 8:0.

only slightly, while the flux passes through a maximum. The same tendencies are observed when increasing the MA content from 0 to 5% (w/w).

Light transmission curves for Me and MA (Figs. 9 and 10) show a remarkable resemblance. For both additives, at zero content hardly any inhomogene-

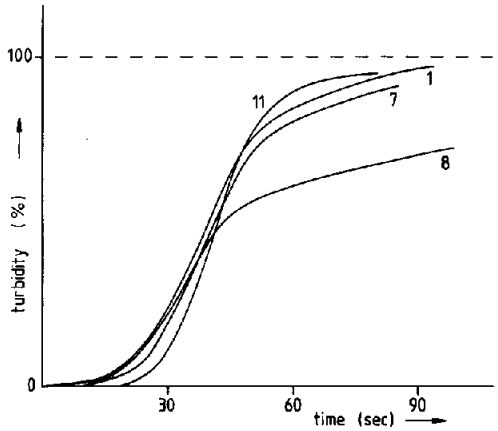

Fig. 9. Light transmission measurements: influence of Me. Numbers refer to the casting solutions (see Table I). 1, 7% (w/w) Me (basic solution); 7, 0% Me; 8, 14% (w/w) Me; 11, 0% Me and 0% MA.

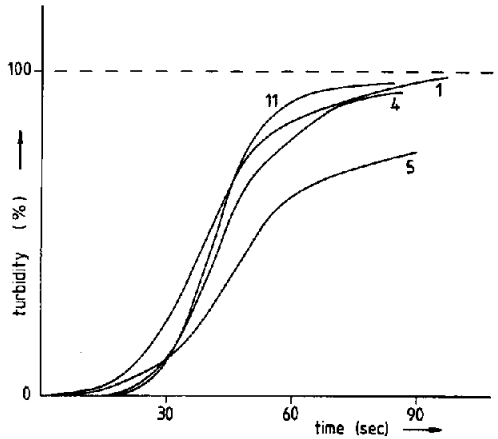

Fig. 10. Light transmission measurements: influence of MA. Numbers refer to the casting solutions (see Table I). 1, 3% (w/w) MA (basic solution); 4, 0% MA; 5, 5% (w/w) MA; 11, 0% MA and 0% Me.

ities (caused by aggregate formation) can be detected (B-type light transmission curve, see Fig. 3a). Consequently, the SEM photographs (Figs. 11, 12) show a homogeneous, dense toplayer, causing a low flux and a high rejection. According to both the light transmission curves and the SEM photographs, enhanced aggregate formation is observed when the additive content is raised. This leads to a more porous structured layer in between the skin and the sublayer, resulting in a lower flux resistance.

When the additive concentration in the casting solution is increased further,

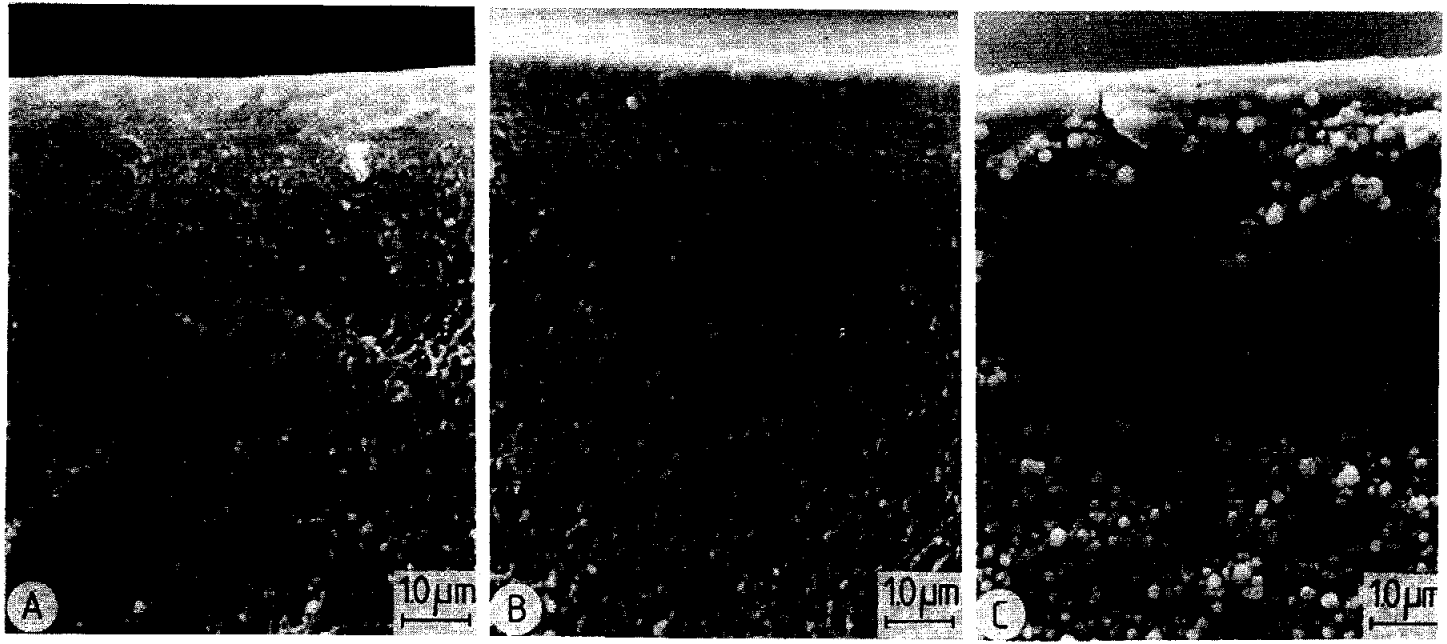

Fig. 11. SEM cross-sections: influence of Me. A, 0% Me; B, 7% (w/w) Me (No. 1 basic solution); C, 14% (w/w) Me.

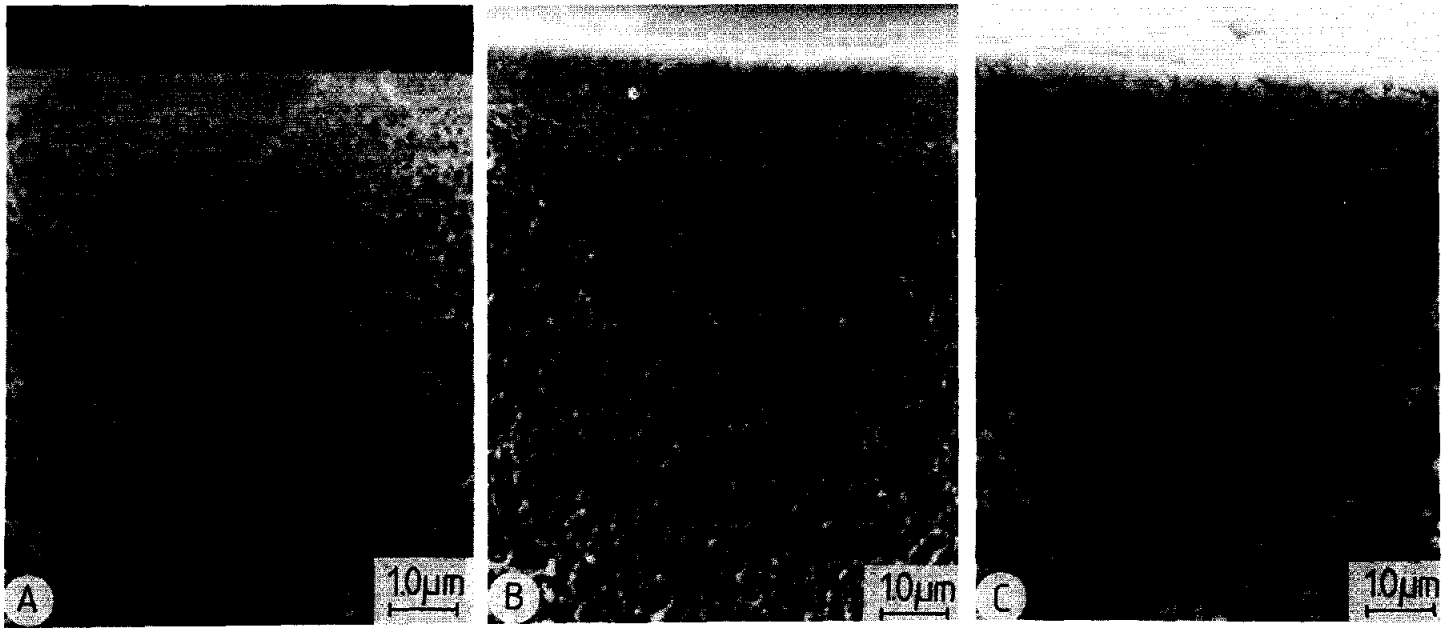

Fig. 12. SEM cross sections: influence of MA. A, 0% MA; B, 3% (w/w) MA (No. 1 basic solution); C, 5% (w/w) MA.

aggregate formation proceeds at a lower rate (according to the light transmission curves 5 and 8 in Figs. 9 and 10), but the layer in which aggregate formation occurs extends to constitute a considerable part of the membrane cross-section (according to the SEM photographs). The role of l–l demixing in structure formation is decreased, which is illustrated by the fact that the membrane formation process ends at a significantly lower turbidity level. An increased outgrowth of the aggregates might lead to a more dense structure which, mostly by means of its thickness, leads to a flux decrease. Thus, the use of Me and MA as additives is characterized by a concentration optimum at which a maximum flux is achieved. Only the flux appears to be strongly dependent on the additive content. The salt rejection is determined mainly by the skin density, which is obviously not affected significantly by the use of additives.

If both Me and MA are omitted, no aggregate formation occurs before l–l demixing begins (Figs. 9 and 10, curve 11). Because of the resemblance between this curve and the curves for zero Me content (Fig. 9, curve 7) and MA (Fig. 10, curve 4), respectively, we expected a similar structure and hence a similar RO performance, i.e. a high rejection and a low flux. However, we obtained membranes with pinhole size voids, which account for the very low rejections (Table III). It seems that at least one of the additives is necessary to avoid pinhole voids.

Further investigation on the role of additives — demixing experiments

We investigated demixing phenomena in the basic coagulation system, i.e. the basic casting solution (No. 1) with water as the coagulation medium. As a simplification, we represent this 7-component system in a ternary diagram (Fig. 13).

We used fixed ratios of CA:CTA and Dio:Ac. Me and MA have not been incorporated in the diagram because their concentrations have been kept constant at 7 and 3% (w/w), respectively. At a constant polymer concentration of 4% (w/w) we made solutions with water contents varying from 20 to 54% (w/w).

At room temperature, l–l demixing only occurred at water contents of 25% (w/w) and higher. At water contents below 25% (w/w) the solutions were slightly turbid, but it was not possible to isolate a clear, homogeneous phase. After some days however, these solutions showed a small amount of precipitate, while the supernatant had remained turbid.

Severe problems were encountered in preparing homogeneous solutions. Clear solutions could neither be obtained by applying high temperatures (up to 80°C), nor by adding the components subsequently, nor by a combination of both. After 5 h at 100°C, only at low polymer concentrations (up to 2.5%, w/w) could clear solutions be obtained which, however, did not show any demixing tendency at temperatures above 0°C. Only after some days, the same kind of

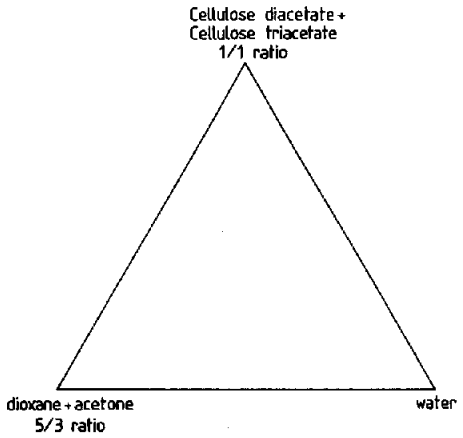

Fig. 13. Simplified representation of the 7-component system in a ternary diagram. Me and MA omitted.

precipitate emerged as in the turbid solutions mentioned earlier. Therefore, no further attempts at homogenization were made: the above mentioned l–l demixing data apply to solutions which have been slightly turbid from the beginning.

The emergence of turbidity, as well as the formation of a precipitate, appeared to be practically irreversible. This means that under reasonable conditions (temperature below 80 °C), the dissolution of the precipitate proceeds at an extremely low rate. The formation of a turbid solution, without l–l demixing taking place, is a well-known phenomenon in the systems CA/Dio/water and especially CA/Ac/water and should be explained by aggregate formation [12]. However, the formation of a solid precipitate has never been observed in these systems. CTA is known to show an increased ability to crystallize, caused by the higher degree of structural regularity compared to CA. This crystallization shows a strong hysteresis, i.e. crystallites are only formed at high degrees of supercooling and after long induction times, while they bearly dissolve at temperatures below 100 °C.

Thus, in this blend system we can expect two different demixing processes to occur during membrane formation:
(1) l–l demixing and (2) aggregate formation, which is strongly inherent to the crystallization of CTA. Attention was paid to the influence of Me and MA on both demixing phenomena.

Interaction between CA and MA with respect to aging phenomena

Especially for those systems which contained MA a quantitative analysis was extremely difficult owing to the occurrence of 'aging phenomena', i.e. irreversible changes which proceed at a strongly temperature dependent rate. After a time period of several weeks (at room temperature) to 1 d (at 80 °C), the

binodal is shifted, causing l–l demixing to occur at lower temperatures [22,23]. At higher MA contents (>6% (w/w)) the solutions even acquire a yellow colour.

Aging has to be distinguished from l–l demixing and aggregate formation by the time scale in which it takes place. Considering this, aging cannot be supposed to play an important role during membrane formation when using fresh casting solutions that have not been heated too intensively. However, cloud-point measurements require a homogenization procedure of at least 8 h at 80°C, causing aging to disturb these measurements. Secondly, the irreversibility of the aging effects implies a chemical modification of the CA.

Therefore, we tried to investigate the interaction of MA with CA. Polymer films (CA and CA:CTA in a 1:1 ratio) were swollen in water which contained 0–10% (w/w) MA. Without MA, CA and the blend showed swelling values of 12.5% and 6.5%, respectively. Adding MA to the water caused the polymer films to take up considerably more water (up to 76.1% of the final film weight) within the same time (4 d). At higher MA concentrations the polymer films dissolved completely. However, in this case the swelling medium had a pH-value of 2 or less, at which acid hydrolysis of the CA occurred. We can conclude that MA acts as a swelling agent, while creating an acid environment in which the CA decomposes and ultimately dissolves.

No swelling experiments could be done on CA films which contained MA, because it appeared impossible to obtain homogeneous films.

Influence of MA on aggregate formation

In the system CA/Dio/water, the addition of 2% (w/w) MA causes aggregate formation to occur at CA concentrations as low as 2% (w/w). Without MA aggregate formation only occurs at CA concentrations of >20% (w/w) [22,23].

In our CA:CTA blend system, MA appeared to act in the same way.

MA behaviour during l–l demixing

To establish preferential occurrence of MA in one of the phases that emerge during l–l demixing, the diluted phase was analysed for MA by titration. Furthermore, membranes were prepared followed by analysis of the coagulation bath. By setting up a mass balance for the whole system, preferential occurrence of MA in the polymer-rich phase was established for both types of experiments. A strong hydrogen bond interaction between MA and CA can be expected, leading to a higher degree of ordering and hence increased aggregate formation. Because of the good solubility of MA in water, the MA may well be removed from the swollen polymer matrix.

Taking the SEM photographs (Fig. 12) into account, we conclude that MA

influences the demixing behaviour, and thus the membrane structure, in such a way as to enhance aggregate formation and to delay l–l demixing. This is confirmed by the light transmission measurements (Fig. 10).

Influence of Me

In the presence of Me, CTA precipitates from a 5% (w/w) solution in a Dio:Ac (ratio 5:3) mixture. Turbid solutions were already obtained at low Me content, whereas l–l demixing only occurred at 45% (w/w) Me. When water was used as a nonsolvent instead of Me, solutions remained clear until l–l demixing started at ca. 25% (w/w) water.

Thus, concerning the CTA, Me is a less pronounced nonsolvent than water. Instead, Me acts on CTA in a similar way as MA acts on CA: it enhances aggregate formation. Probably because of the relatively high molecular weight of CTA compared to CA, the CTA aggregates are more dense and they even precipitate.

CONCLUSIONS

Wet–dry reversible membranes can be obtained by using a CA:CTA blend as the polymer and by using a two-bath coagulation procedure. The *casting solution* contains about 14% (w/w) of the polymer blend, less than 14% (w/w) Me and less than 5% (w/w) MA, completed by a 5:3 Dio:Ac mixture as the solvent. *Coagulation* is performed using a 0°C water bath (residence time between 30 s and 5 min) and a 60°C water bath (residence time 10 min), consecutively. Using this method, wet–dry reversible membranes with salt rejections of 98–99% and flux values of 10–12 l/m^2 h are obtained with good reproducibility. These desalination properties, combined with a good wet–dry reversibility, make our membranes superior to RO membranes hitherto produced. The flux may be optimized further by varying the Me content around 7% (w/w) and the MA content around 3% (w/w), and by applying a residence time in the first coagulation bath of approximately 30 s.

When one of the components is omitted from the casting solution, the above mentioned membrane properties cannot be obtained. Both MA and Me stimulate aggregate formation. Only if limited amounts of these components are added to the casting solution, aggregate formation results in a slightly porous layer directly below the skin, which is thin enough not to provide too high a flux resistance. The use of the first and second coagulation bath is necessary to obtain a high rejection and a reasonable flux and reproducibility, respectively. The second bath has a remarkable heat curing effect. In the meantime, coagulation may still proceed providing a pore-enlarging effect, especially in the sublayer.

Further investigations can be carried out by varying the temperature of the second bath.

ACKNOWLEDGEMENTS

We wish to thank Steven Groot Wassink for carrying out the demixing experiments and Bart Reuvers for the stimulating discussions. These investigations were supported in part by the International Atomic Energy Agency.

REFERENCES

1 W. Kaiser and F. Schwarzer, Canad. Patent 974718, (1975).
2 W. MacDonald, S. Park and Chuen-Yong Pan, U.S. Patent 3,842,515 (1974).
3 P. Manos, U.S. Patent 4,068,387 (1978).
4 Hitachi, Ltd., Jpn. Kokai, 81,07,602 (1981).
5 W.V. Titov, Brit. Patent 1,305,385 (1973).
6 T. Kawabata, E. Kawaguchi, H. Okada and K. Ikeda, Jpn. Kokai 78,39,272 (1978).
7 T. Asada, F. Komatsu, H. Tsuge, C. Yanagi and T. Kuwahara, U.S. Patent 3,917,777 (1975).
8 R.E. Kesting, U.S. Patent 3,884,801 (1975).
9 M.A. Justice and J.W. McCutchan, U.S. Patent 3,666,508 (1972).
10 Wafilin B.V., Neth. Appl. 78,12,664 (1979).
11 R.E. Kesting, Synthetic Polymeric Membranes, McGraw Hill, New York, 1971.
12 A.J. Reuvers, F.W. Altena and C.A. Smolders, Demixing and gelation behavior of ternary cellulose acetate solutions, J. Polym. Sci. Pol. Phys., in press.
13 M.H.V. Mulder, Internal Report Twente University, 1976.
14 C.R. Canon, U.S. Patent 3,497,072 (1970).
15 R.E. Kesting, in S. Sourirajan (Ed.), Reverse Osmosis and Synthetic Membranes, NRCC, Ottawa, 1977, pp. 89–94.
16 W.M. King, D.L. Hoernschemeyer and C.W. Saltonstall, Jr., in H.K. Lonsdale and H.E. Podall (Eds.), Reverse Osmosis Membrane Research, Plenum, New York, 1972, pp. 131–161.
17 S.V. Joshi and D.J. Mehta, Blended membrane for desalination by reverse osmosis, Indian Chem. J., 12, No. 4 (1977) 22.
18 S. Sourirajan and B. Kunst, in S. Sourirajan (Ed.), Reverse Osmosis and Synthetic Membranes, NRCC, Ottawa, 1977, pp. 147–148.
19 S. Manjikian, S. Loeb and J.W. McCutchan, Improvement in Fabrication Techniques for Reverse Osmosis Desalination Membranes. Proc. 1st Int. Symp. Water Desalination, 1965, pp. 159–173.
20 A.J. Reuvers and C.A. Smolders, Formation of membranes by means of immersion precipitation, part I, submitted for publication in J. Membr. Sci.
21 A.J. Reuvers and C.A. Smolders, Formation of membranes by means of immersion precipitation, part II, submitted for publication in J. Membr. Sci.
22 J.A. Ronner and C.A. Smolders, Investigation of liquid/liquid demixing and aggregate formation in a membrane-forming system by means of pulse induced critical scattering (PICS), J. Membr. Sci., in press.
23 H. Bokhorst, F.W. Altena and C.A. Smolders, Formation of asymmetric cellulose acetate membranes, Desalination, 38 (1981) 349–360.